Design of an electro-optic bunch length monitor for the CERN-CTF3 probe beam

R. Pan,[1,2] T. Lefevre,[1] S. P. Jamison,[3] and W. A. Gillespie[2]

[1] *Beam Department, the European Organization for Nuclear Research, CH-1211 Geneva 23, Switzerland*
[2] *Carnegie Laboratory of Physics, University of Dundee, Dundee DD1 4HN, United Kingdom*
[3] *Accelerator Science and Technology Center, STFC Daresbury Laboratory, Warrington WA4 4AD, United Kingdom*

(Dated: January 23, 2012)

One of the most promising devices to provide accurate measurements of the longitudinal beam profile for CLIC is based on electro-optic techniques. A bunch length monitor, based on electro-optic spectral decoding (EOSD), is currently being designed for the CLIC Test Facility 3 at CERN. EOSD encodes the Coulomb field profile of a bunch onto a time-wavelength correlated optical probe, with the temporal profile of the bunch subsequently read-out through the wavelength spectrum of the optical probe. The detector will be installed on CALIFES, the CTF3 probe beam, which typically provides bunches with a charge of 0.6 nC and a bunch length of 1 ps r.m.s. This paper gives an overview of the proposed detection schemes, which have been investigated and evaluated. Our final choice are presented .

PACS numbers: 41.85.Ew, 42.65.Re, 41.75.Ht

I. INTRODUCTION

A 3 TeV e^+e^- Compact Linear Collider (CLIC) is currently being studied at CERN [1]. CLIC is based on the two-beam acceleration scheme in which drive beams with high current and high frequency are continuously decelerated to provide the required RF power for accelerating the colliding beams. To reach high luminosity the machine relies on colliding beams with nanometre transverse sizes. The bunch length must also be kept short to avoid any luminosity dilution [2]. It is to be compressed down to 150 fs rms just before the CLIC main linac, and the longitudinal profile must be measured with a resolution of 20 fs. Only very few instruments can provide longitudinal profile measurement with femtosecond time resolution. The resolution of deflecting cavities has already been demonstrated better than 10 fs [3][4], but the measurements are destructive. Moreover, to reach similar resolution on high energy beams ($>$ 100 GeV) the devices would require the use of extremely high radiofrequency power or a very long deflecting cavity, which might not be practical.

A non-intercepting solution can be based on the Electro-Optic (EO) technique [5]. This is based on the polarization change of a laser beam which passes through a birefringent crystal itself polarized by the Coulomb field of the electron beam. The first demonstration of EO sampling [6] for electron bunch length measurement was done at FELIX, the FEL facility in the Netherlands. During the following years, EO single shot techniques were introduced and have now been demonstrated on several accelerators and in many distinct forms, such as EO Spectral Decoding (EOSD) [7], EO Spatial Encoding (EOSE) [8], EO Temporal Decoding (EOTD) [9] and EO spectral upconversion [10]. EOTD encodes the beam longitudinal profile onto the temporal profile of a several ps long optical pulse, and reads it out through a time-space mapping in an optical cross-correlator. This technique provides the best performance among all the EO techniques for measuring a bunch of 120 fs rms. EOSD encodes the bunch Coulomb field profile on to a time-wavelength correlated optical probe. The temporal profile is read out by measuring the frequency spectrum of the laser probe. It does not provide the best temporal resolution but has shown its capability to work reliably in the picosecond regime.

At CERN, some of the key feasibility issues of CLIC are currently being studied at CLIC Test Facility 3 (CTF3) [11]. Even if CTF3 cannot provide electron bunches as short as 150 fs rms, the CTF3 probe beam, named Califes [12], typically runs with bunches of 1 ps or below. This paper presents the design of a picosecond longitudinal profile monitor based on EOSD to be installed on the Califes beam line.

II. CALIFES

The layout of the CALIFES beam line is depicted in FIG. 1. The accelerator is composed of one photoinjector, three travelling-wave structures, and one section equipped with beam diagnostics. The beam is then sent into the two-beam test stand where it is accelerated in CLIC-type accelerating structures. The photoinjector uses a Cs_2Te photocathode illuminated by 262 nm laser pulses [13][14]. Typical bunches in CALIFES have a charge ranging from 85 to 600 pC depending on the laser pulse energy and the quantum efficiency of the photocathode. The electron bunch length, initially of 5 ps, is compressed using velocity bunching in the first accelerating structure and in normal conditions the bunches at the end of the linac are as short as 1.4 ps r.m.s. The machine can be run either in a single bunch mode, or a multi bunch mode with a typical pulse train consisting of 226 bunches over 150 ns at 5 Hz repetition rate. The RF system of Califes relies on a single klystron equipped with pulse compression and providing an RF pulse of 45 MW within 5.5 μs. The beam energy can reach up to

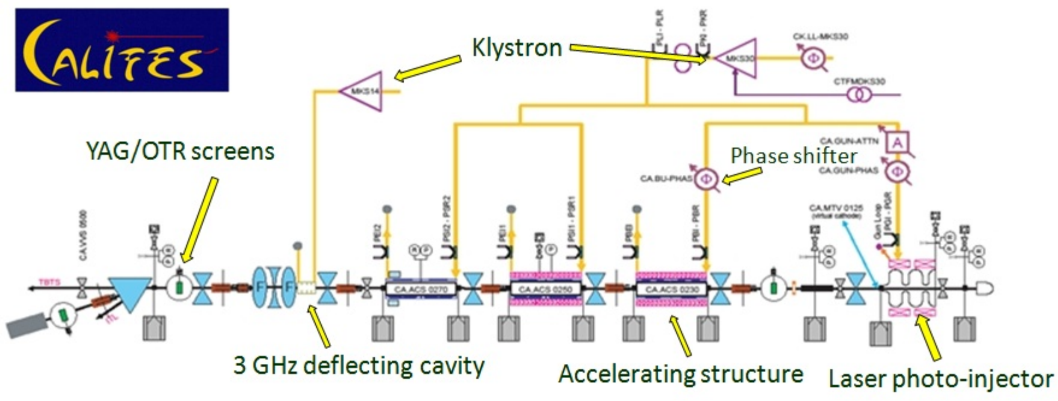

FIG. 1. (Color online) CALIFES layout

200 MeV at the end of the linac. Immediately afterwards, the beam enters a diagnostic section including emittance, bunch length and energy spread measurements.

There are two bunch length monitors installed on CALIFES [15]. One uses a deflecting cavity driven by an additional klystron. When the beam passes through the cavity, the particles experience a time-varying kick. The longitudinal profile of the beam is thus transformed into a transverse profile and can be measured by an OTR screen downstream. The other monitor measures the beam energy dispersion introduced intentionally by the CLIC acceleration in the two-beam test stand. When the beam goes through the accelerating structure, the particles experience a time-varying acceleration (or deceleration) depending on the relative phase difference between the RF and the beam. The corresponding increase in energy spread is measured in a spectrometer line and provides a measurement of the bunch longitudinal profile. However, these two monitors require either the presence of the drive beam to power the accelerating structure or an extra driving klystron which is currently used for the regular operation of the CTF3 drive beam. There is then a strong requirement to build a dedicated bunch profile monitor for CALIFES.

III. DESIGN OF AN EO SPECTRAL DECODING SYSTEM FOR CALIFES

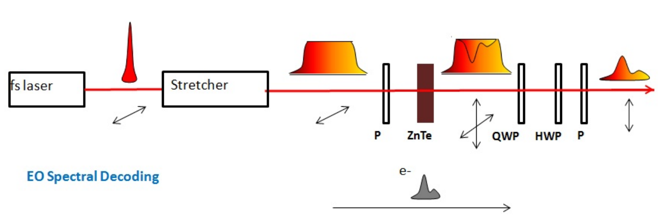

FIG. 2. (Color online) Scheme for EOSD setup

The principle of operation of an Electro-Optical spectral decoding longitudinal profile monitor is shown in FIG. 2. It encodes the Coulomb field of an e-bunch into a linearly chirped broadband laser pulse. Since the laser is chirped linearly, the frequency components of laser pulse are equally distributed in time. When the Coulomb field and laser pulse go through the crystal simultaneously, the polarization of the laser pulse varies with the amplitude of Coulomb field. A pair of crossed polarizers are put on both sides of the crystal in order to transfer the polarization variation into a laser intensity variation. The bunch profile information is thus encoded in the chirped laser pulse both in time domain and frequency domain. To extract the bunch profile information, a frequency spectrometer using a grating converts the spectrum of the laser pulse into a transverse profile, which is then detected by a high sensitivity CCD camera.

The monitor measures the Coulomb field of the electron bunch. The profile similarity between Coulomb field and electron bunch depends on beam energy which can strongly impact on the absolute time resolution of the monitor. For a non-relativistic particle, the Coulomb field is homogenenously distributed around the particle and will not be representative of the bunch longitudinal profile. However, when the electron is moving close to the velocity of light, its Coulomb field is compacted, perpendicular to its direction of propagation with an opening angle $\theta = \frac{2}{\gamma}$ [16]. At very high energy, the opening angle becomes so small that the profile of the Coulomb field becomes an almost perfect replica of the bunch temporal profile. The Coulomb field of the bunch can be described as follows

$$E_{\mathrm{Colm}}(r,t) = E_{\mathrm{e0}}(r,t) * \rho(r,t) \tag{1}$$

where ρ describes the electron density distribution, and the Coulomb field of one electron E_{e0} is given by:

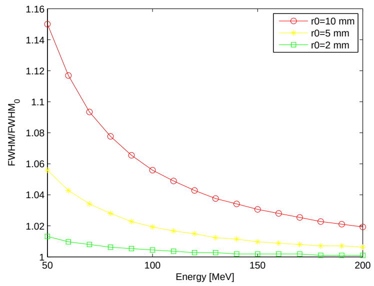

(a)Relative increase in Coulomb field duration as function of beam energy

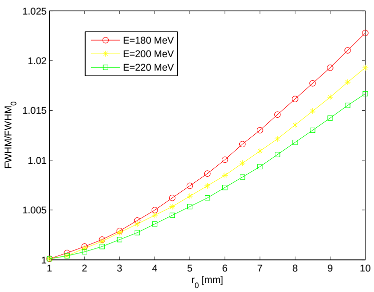

(b)Relative increase in Coulomb field dutation as function of radial offset

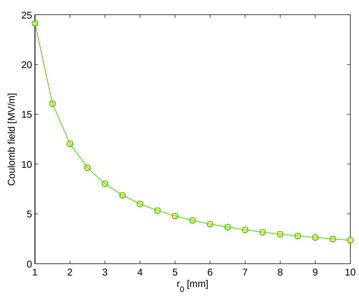

(c)Coulomb field amplitude vs. radial offset

FIG. 3. (Color online) Simulation for Coulomb field

$$E_{\mathrm{e0}}\left(r_0,t\right)=\frac{e_0\gamma}{4\pi\epsilon_0}\cdot\frac{r_0}{\left(r_0^2+\gamma^2\nu_{\mathrm{e}}^2\left(t-t_0\right)^2\right)^{3/2}} \quad (2)$$

where γ is Lorenz factor, and r_0 is the radial displacement from the beam propagation path.

Fig. 3 shows the broadening of the Coulomb field with a bunch of 1.4 ps FWHM as a function of the beam energy and the distance between the beam and the crystal. In FIG. 3(a) it can be seen that the difference between the length of Coulomb field and the length of e-bunch temporal profile is quite small for high energy beams. There is only 1% broadening for a 200MeV beam and a crystal positioned at 5 mm from the beam. The beam is assumed to be entirely on-axis, with no radial extent. The time resolution of the monitor will improve as the crystal is moved closer to the beam, as shown in FIG. 3(b). FIG. 3(c) shows the amplitude of the Coulomb field for different distances of the crystal from the e-bunch. The optimum distance for the crystal would depend on a compromise between the expected time resolution, the signal to noise ratio of the monitor and the risk of damaging the crystal if the beam directly impinges on it. In the case of CALIFES, a distance between 5-10mm seems to be a reasonable choice.

The core component of the EOSD system is the two-crossed-polarizer setup. It contains a polarizer, EO crystal, a quarter wave plate (QWP), a half wave plate (HWP) and another polarizer which is crossed with respect to the previous one. The EO crystal induces a frequency mixing between the Coulomb field and laser pulse due to its non-linear coefficient. A combination of QWP and HWP can compensate the residual birefringence in the EO crystal and adjust the background in the final signal. Using a Jones matrix formalism, the output electric field polarisation can be described by the following matrix:

$$E_{\mathrm{Out}}\left(\omega\right)=\left[\begin{array}{cc}0&1\end{array}\right]R\left(\varphi\right)M_{\mathrm{H}}R\left(-\varphi\right)R\left(\alpha\right)M_{\mathrm{Q}}R\left(-\alpha\right)R\left(\theta\right)M_{\mathrm{EO}}R\left(-\theta\right)\left[\begin{array}{c}E_{\mathrm{Laser}}^{\mathrm{Chirp}}\left(\omega\right)\\0\end{array}\right], \quad (3)$$

where the $R\left(\theta\right)$ is rotation matrix, M_{H} and M_{Q} are Jones matrices for HWP and QWP respectively. The frequency mixing in the EO crystal is described in M_{EO} matrix as [17]:

$$M_{\mathrm{EO}}=\left[\begin{array}{cc}\left(1+\frac{i\omega}{2nc}\cdot\widetilde{E}_{\mathrm{Coul}}^{Eff}*\right)&0\\0&\left(1-\frac{i\omega}{2nc}\cdot\widetilde{E}_{\mathrm{Coul}}^{Eff}*\right)\end{array}\right] \quad (4)$$

$$\text{where } \widetilde{E}_{\mathrm{Coul}}^{Eff}\left(0,\Omega\right)=\chi_{Eff}^{(2)}\left[\frac{e^{i\Delta k(\omega,\Omega)z}-1}{i\Delta k\left(\omega,\Omega\right)}\right]\cdot\widetilde{E}_{\mathrm{Coul}}\left(0,\Omega\right) \quad (5)$$

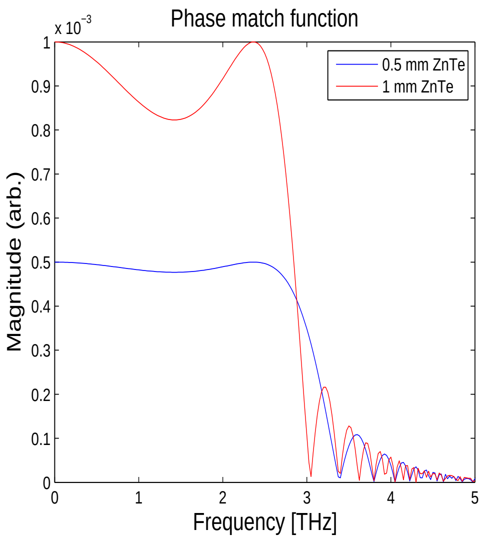

(a)ZnTe (0.5mm and 1mm thickness)

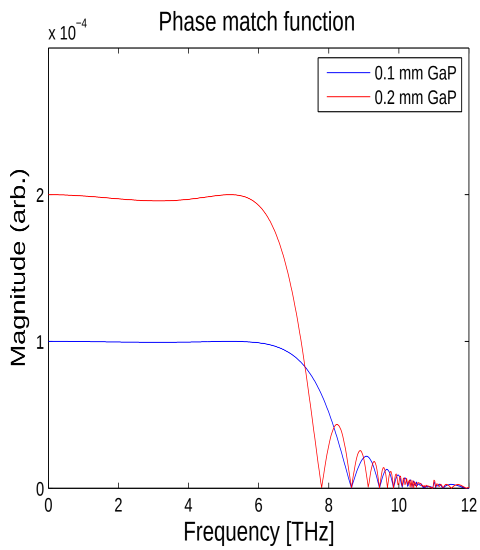

(b)GaP (0.1mm and 0.2mm thickness)

FIG. 4. (Color online) Magnitude of phase match functions

where Ω is the frequency of Coulomb field, n is laser wavelength refraction index in the crystal. $\widetilde{E}^{Eff}_{\text{Coul}}(0,\Omega)$ is the effective Coulomb field. It includes the nonlinear coefficient of the EO crystal and the phase matching term which can be seen in equation 5. The frequency response of the EO crystal due to the phase matching is shown in FIG. 4. With a wider frequency response range, the bunch profile will be retrieved with a better time resolution.

The frequency response for the ZnTe crystal is depicted in FIG. 4(a). For a 1 mm thick crystal, the cut off frequency corresponds to 3 THz. The frequency response also reduces with thicker crystals because of the phase mismatch between the Coulomb field and the laser field. Better time resolution would be obtained by using a GaP crystal as shown in FIG. 4(b). The frequency response of a 100 um GaP extends up to 8.5 THz.

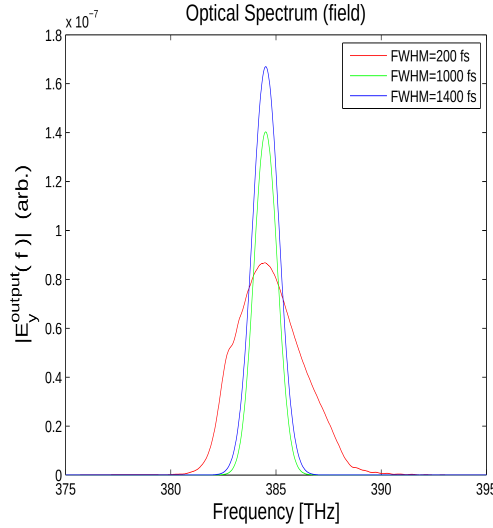

(a)Simulation of measured signal for 200fs, 1000fs, 1400fs bunches

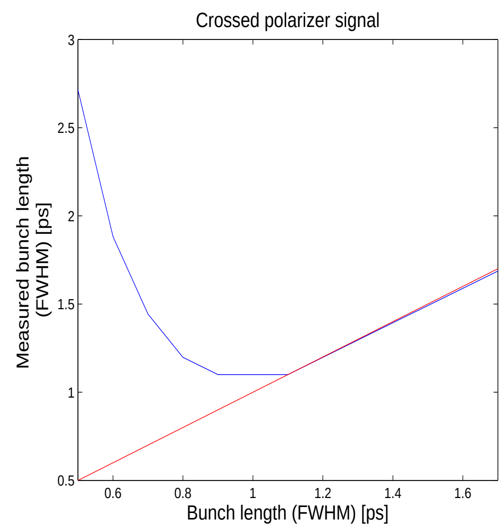

(b)EOSD limitation

FIG. 5. (Color online) EOSD results (laser wavelength=780nm, pulse duration=150fs, crystal=500μm ZnTe, distance=5mm)

Based on Equation 1–5, the simulated output signal emerging from the last polarizer for different duration Guassian bunches are shown in FIG. 5(a). It shows how well the real beam profile is reconstructed using a 500 um thick ZnTe crystal. For 200 fs bunches, the signal is strongly distorted. It leads to a large broadening of the measured profile (the red curve in FIG. 5(a)). The reason of this distortion is that the short pulse induces a fast temporal modulation in the crystal, and the spectral content of the fast modulation distorts the time-wavelength mapping of the laser pulse which leads to a broadening. This is the main limitation of EOSD, shown in FIG. 5(b), and can be calculated by $\tau_{lim} \approx \sqrt{\tau_0^{FWHM}\tau_c^{FWHM}}$, depending on the duration of original and chirp laser pulses [18].

The laser is also an important component of the EOSD system. Its stability and pulse duration can directly affect the quality of the final measured signal. Laser pulse energy directly impacts on the final signal to noise ratio of the measurement. The intensity of the measured signal depends on the intensity of the Coulomb field (i.e. bunch charge and beam energy), the characteristics of the EO crystal and the sensitivity of the camera. In previous EOSD experiments, the minimum laser pulse energy was 1.5 nJ at 1030 nm to measure the profile of a 50 pC e-bunch using a 500 μm thick GaP crystal [19]. Similarly, 4 nJ laser pulse energy at 800 nm wavelength was used to measure a 0.5 to 1 nC bunch charge with a 65 um thick GaP crystal [20].

The wavelength of the laser must be chosen appropriately to minimize pulse distortion due to phase-matching in the EO crystal. 1030 nm wavelength is usually preferred for GaP and 800 nm for ZnTe. As mentioned previously, the thickness of the crystal also plays an important role for getting optimum phase matching. Typically crystal thicknesses should be thinner than 200 um for GaP and 4 mm for ZnTe to achieve best time resolution. However the laser amplitude to be detected after the crossed polarizers is directly proportional to the thickness and the electro-optical coefficient of the crystal. The coefficients [21] are 0.97 and 3.9 pm/V respectively for GaP and ZnTe, which makes ZnTe an appropriate choice for better signal to noise ratio at the price of limited time resolution. The SNR can be recovered if using lasers with high pulse energy and a very sensitive camera. In Table I, estimations of the EOSD expected performance are presented considering different crystals and commercially available laser systems.

Compared with other EO techniques, EOSD has the lowest laser pulse energy requirement. The EO monitor based on EOSD can be achieved with a commercial fibre laser. It can also provide a subpicosecond resolution which is suitable for the beam in CALIFES. Four commecial fibre lasers were considered in this study. Laser options 1 and 2 are standard ytterbium and erbium fibre lasers respectively. Although higher laser pulse energies are available from the ytterbium laser, they would imply using a GaP crystal which has a lower EO coefficient. Also as shown in the table, higher generated nonlinear energies are easily obtained if using an erbium laser and ZnTe crystal. Laser option 3 is an Er laser with 20 m fibre link between oscillator and amplifier. With the lower coupling efficiency of the PM fibre, one third of laser energy might be lost. Laser option 4 is an Er laser with a pulse picker between oscillator and amplifier. Its repetition rate can be reduced from 75 MHz down to 37.5 MHz or even lower to enhance the pulse energy. The expected final output pulse energy could reach 2.7 nJ. To select the appropriate laser for our system, four commerieally available lasers have been considered, with laser pulse energy and wave length as shown. The choice of GaP or ZnTe crystal is dependent on the laser wavelength and phase-matching constraints. The final column of Table I gives the pulse energy expected in a 'crossed polariser' configuration at Coulomb field strengths of 600 pC. The every contained with the 'crossed polariser' signal shown in the final column of the table. This value is taken as the figure of merit for signal perfomance. The precise value of this figure of merit depends on chirp, and in our case a chirped pulse duration of 3 ps is assumed. With shown the highest non-linear generated pulse energy, the option 4 has been chosen for CALIFES finally.

IV. IMPLEMENTATION OF THE EO MONITOR IN CTF3

Considering the radiation level close to the accelerator, it was decided to keep the laser far away from the accelerator. It will be housed in an optical laboratory located in a technical gallery, roughly 20 metres away from the machine. The detection system including the grating and the camera will also be installed in the laser laboratory. The implementation of the system in CALIFES is presented in Fig 6.

The laser is locked to a 74.963 MHz external RF signal derived from the radiofrequency system of the accelerator. The timing between laser pulse and e-bunch will be adjusted by a RF phase shifter and an optical delay stage. The laser is then stretched to several picoseconds by two gratings and is sent down to the accelerator hall using an in-air optical transport line. Two vacuum chambers are required in the proposed set-up. The first chamber, equipped with a mirror is used to inject the laser into the beam pipe. The second chamber will house the crystal and an extra mirror. The two vacuum chambers will be equipped with a motorized translation stage to precisely position the crystal and mirrors inside the beam pipe. The second chamber will also be equipped with an Optical Transition Radiation screen, which will enable us to check the timing difference between the electron bunch and the laser pulse using a streak camera. The blue mirror mounts in FIG. 6 are picomotor mirror mounts which are used to adjust the laser path remotely. Six pinhole cameras will be used to observe the laser path. There is a half waveplate (HWP) before the first chamber and a HWP and a quarter waveplate (QWP) after the second chamber. The first HWP is used to change the laser polarization and the second HWP and the QWP are used to compensate the residual birefringence induced by the EO crystal. The three wave plates are mounted in motorized rotation stages. All the picomotor mirror mounts and rotation stages can be controlled locally from the laser room. The motors in the two vacuum chambers will be controlled via the CTF3 control system so that it can be accessible from any computer. After emerging from the vacuum chamber, the laser is steered through waveplates and polarizer, and then coupled into a fibre.

TABLE I. Laser performance comparison

Laser	Wavelength(mm)	Input Pulse Energy(nJ)	Crystal	Crystal Thickness(μm)	EO Coefficient(pm/V)	Non-linear Generated Pulse Energy(pJ)
1	1030	10	GaP	200	0.97	0.118
2	780	1.8	ZnTe	1000	3.9	0.9
3	780	1.2	ZnTe	1000	3.9	0.6
4	780	2.7	ZnTe	1000	3.9	1.37

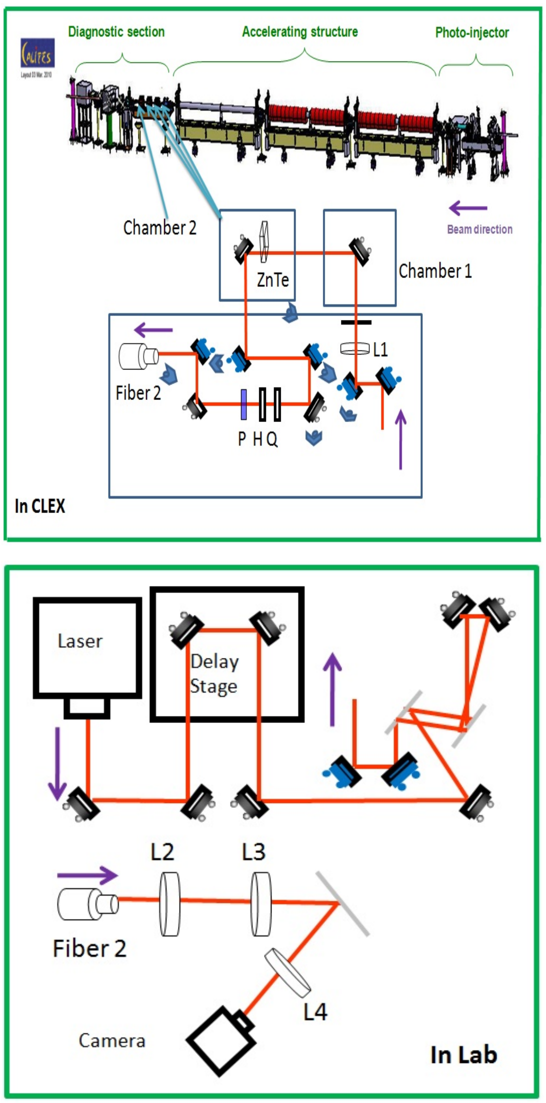

FIG. 6. (Color online) EO monitor scheme

The fibre is linked back to the laser room. Finally, the spectrum of the final laser pulse is measured by a grating spectrometer and detected by a gated ICCD camera. A few beam loss monitors will also be installed around the crystal vacuum chamber to check that the beam or beam halo are not impinging directly on the crystal.

V. RESOLUTION

The resolution of the EOSD system can be evaluated by the following:

- Distance between crystal and e-bunch: for 5 mm distance between crystal and e-bunch, the resolution limit imposed by the Coulomb field spread will be approximately 10 fs.
- Frequency response of crystal (material and thickness): the cut off frequency of ZnTe crystal is around 3 THz at the thickness of 1 mm, so the resolution limit induced by phase matching will be approximately 330 fs.
- Laser pulse duration and chirp duration: when the length of the electron bunch is too short, a distortion appears in the spectrum of the output signal. Our laser pulse is 100 fs and will be chirped to 3 ps, giving a limiting duration of the bunch of approximately 550 fs for EOSD.
- Resolution of spectrometer and CCD: assuming a spectrometer resolution limited by the pixel size of detector, we estimate a resolution limit as follows. A wavelength range of 20 nm covers the detector array of 1000 pixels. With a chirp of 3 ps, the 0.02 nm pixel gives a resolution of 3 fs.

Therefore the resolution of our EO monitor is expected to be sub-picosecond.

VI. SUMMARY

A longitudinal profile monitor for the CALIFES beam (200 MeV, 0.6 nC/bunch) has been proposed and is currently under construction. It is based on the Electro-Optical spectral decoding technique and is aimed at providing measurements with a time resolution better than 1ps. Numerical simulations have been performed to define and optimize the main components of the system.

Our choice has favoured a solution with an optimum signal to noise ratio. We choose to start with a 1 mm thick ZnTe crystal and an Er fibre laser with a pulse picker providing 2.7 nJ output pulse energy at 780 nm and a 120 fs pulse duration. The implementation of the EO bunch length monitor system has been studied in detail and the main components are currently being ordered and constructed. The laser and camera will be kept in a dedicated laser laboratory to avoid any radiation damage. The two-crossed-polarizer set up will sit in the machine close to the beam. The resolution of this system is expected to be in the sub-picosecond range. The installation of the monitor will start in early 2012 and a first test is expected to be performed by the end of the summer.

ACKNOWLEDGMENTS

This research project has been supported by a Marie Curie Early Initial Training Network Fellowship of the European Community's Seventh Framework Programme under contract number (PITN-GA-2008-215080-DITANET)

[1] T. C. S. Team, *A 3 TeV e^+e^- Linear Collider Based on CLIC Technology*, Tech. Rep. (CERN, 2000).

[2] H. Braun, R. Corsini, J.-P. Delahaye, A. D. Roeck, S. Doebert, G. Geschonke, A. Grudiev, C. Hauviller, B. Jeanneret, E. Jensen, T. Lefevre, Y. Papaphilippou, G. Riddone, L. Rinol, W.-D. Schlatter, H. Schmickler, D. Schulte, I. Syratchev, M. Taborelli, F. T. (editor), R. Tomas, S. Weisz, and W. Wunsch, *CLIC 2008 PARAMETERS*, CLIC-Note-764 (CERN, Switzerland, October 2008).

[3] G. Berden, W. A. Gillespie, S. P. Jamison, E. Knabbe, A. M. MacLeod, A. F. G. van der Meer, P. J. Phillips, H. Schlarb, B. Schmidt, P. Schmuser, and B. Steffen4, Physical Review Letters **99**, 164801 (2007).

[4] K. Bane, F. Decker, Y. Ding, D. Dowell, P. Emma, J. Frisch, Z. Huang, R. Iverson, C. Limborg-Deprey, H. Loos, H.-D. Nuhn, D. Ratner, G. Stupakov, J. Turner, J. Welch, and J. Wu, Physical Review Special Topics - Accelerators and Beams **12**, 030704 (2009).

[5] S. Jamison, G. Berden, A. MacLeod, B. Steffen, P. J. Phillips, and W. Gillespie, in *Proceedings of EPAC 2006* (Edinburgh, Scotland, 2006) p. 915.

[6] X. Yan, A. M. MacLeod, W. A. Gillespie, G. M. H. Knippels, D. Oepts, A. F. G. van der Meer, and W. Seidel, Physical Review Letters **85**, 3404 (2000).

[7] I. Wilke, A. M. MacLeod, W. A. Gillespie, G. Berden, G. M. H. Knippels, and A. F. G. van der Meer, Physical Review Letters **88**, 124801 (2002).

[8] A. Azima, S. Dusterer, H. Schlarb, J. Feldhaus, A. Cavalieri, D. Fritz, and K. Sengstock, in *Proceedings of EPAC 2006* (Edinburgh, Scotland, 2006) p. 71.

[9] G. Berden, S. P. Jamison, A. M. McLeod, W. A. Gillespie, B. Redlich, and A. F. G. van der Meer, Physical Review Letters **93**, 114802 (2004).

[10] S. P. Jamison, G. Berden, P. J. Phillips, W. A. Gillespie, and A. M. MacLeod, Applied Physics Letters **96**, 231114 (2010).

[11] G. Geschonke and A. G. EDs, *CTF3 Design Report*, CERN/PS 2002-008(RF) (CERN, Switzerland, 2002).

[12] A. Mosnier, M. Authier, D. Bogard, A. Curtoni, O. Delferriere, G. Dispau, R. Duperrier, W. Farabolini, P. Girardot, M. Jablonka, J.-L. Jannin, M. Luong, and F. Peauger, in *Proceedings of the EPAC 2006* (Edinburgh, Scotland, 2006) p. 679.

[13] J. Brossard, M. Desmons, B. Mercier, C. Prevost, and R. Roux, in *Proceedings of the EPAC 2006* (Edinburgh, Scotland, 2006) p. 828.

[14] M. CsatariDivall, A.Andersson, B.Bolzon, E.Bravin, E.Chevallay, S.Dobert, A.Drozdy, V.Fedosseev, C. Hessler, T.Lefevre, S.Livesley, R.Losito, O. Mete, M.Petrarca, and A.N.Rabiller, Nuclear Instruments and Methods in Physics Research **A659**, 1 (2011).

[15] W. Farabolini, C. Simon, F. Peauger, A. Curtoni, D. Bogard, P. Girardot, M. Csatari, N. Lebas, M. Petrarca, E. Chevallay, R. Ruber, A. Palaia, and V. Ziemann, in *Proceedings of Linear Accelerator Conference LINAC2010* (Tsukuba, Japan, 2010) p. 46.

[16] J. D. Jackson, *Classical Electrodynamics*, 3rd ed. (John Wiley and Sons, Inc., 1999).

[17] S. P. Jamison, A. M. MacLeod, G. Berden, D. A. Jaroszynski, and W. A. Gillespie, Optics Letters **31**, 1753 (2006).

[18] S. Jamison, G. Berden, W. Gillespie, P. Phillips, and A. MacLeod, in *Proceedings of EPAC08* (Genoa, Italy, 2008) p. 1149.

[19] J. Breunlin, *Commissioning of an Electro-Optic Electron Bunch Length Monitor at FLASH*, Master's thesis, University Hamburg (2011).

[20] B. Steffen, V. Arsov, G. Berden, W. A. Gillespie, S. P. Jamison, A. M. MacLeod, A. F. G. van der Meer, P. J. Phillips, H. Schlarb, B. Schmidt, and P. Schmuser, Physical Review Special Topics - Accelerators and Beams **12**, 032802 (2009).

[21] A. Yariv, *Quantum electronics*, 2nd ed. (John Wiley and Sons, Inc., 1989).